

Supporting Information

A Synergetic Enhancement Strategy of Light Utilization and Carrier Transfer for UV Photodetection Associated with the Artificial Resonance Nano-Cavities

Zhenpeng Cheng,^a Zeping Li,^a Ming-Yu Li,^{*a} Xiaoyan Wen,^a Xumin Ding,^b Hao Xu,^c Jihoon Lee,^d Haifei Lu^{*a} and Sisi Liu^{*a}

^aSchool of Science, Wuhan University of Technology, Wuhan, 430070, China

^bAdvanced Microscopy and Instrumentation Research Center, School of Instrumentation Science and Engineering, Harbin Institute of Technology, Heilongjiang, 150001, China

^cSchool of Physics, University of Electronic Science and Technology of China, Chengdu, 611731, China

^dDepartment of Electronic Engineering, College of Electronics and Information, Kwangwoon University, Nowon-gu, Seoul 01897, Republic of Korea

*Corresponding authors. E-mail: mingyuli.oliver@gmail.com (Ming-Yu Li), haifeilv@whut.edu.cn (Haifei Lu), liusisi0109@hotmail.com (Sisi Liu)

Supplementary Figures and Tables

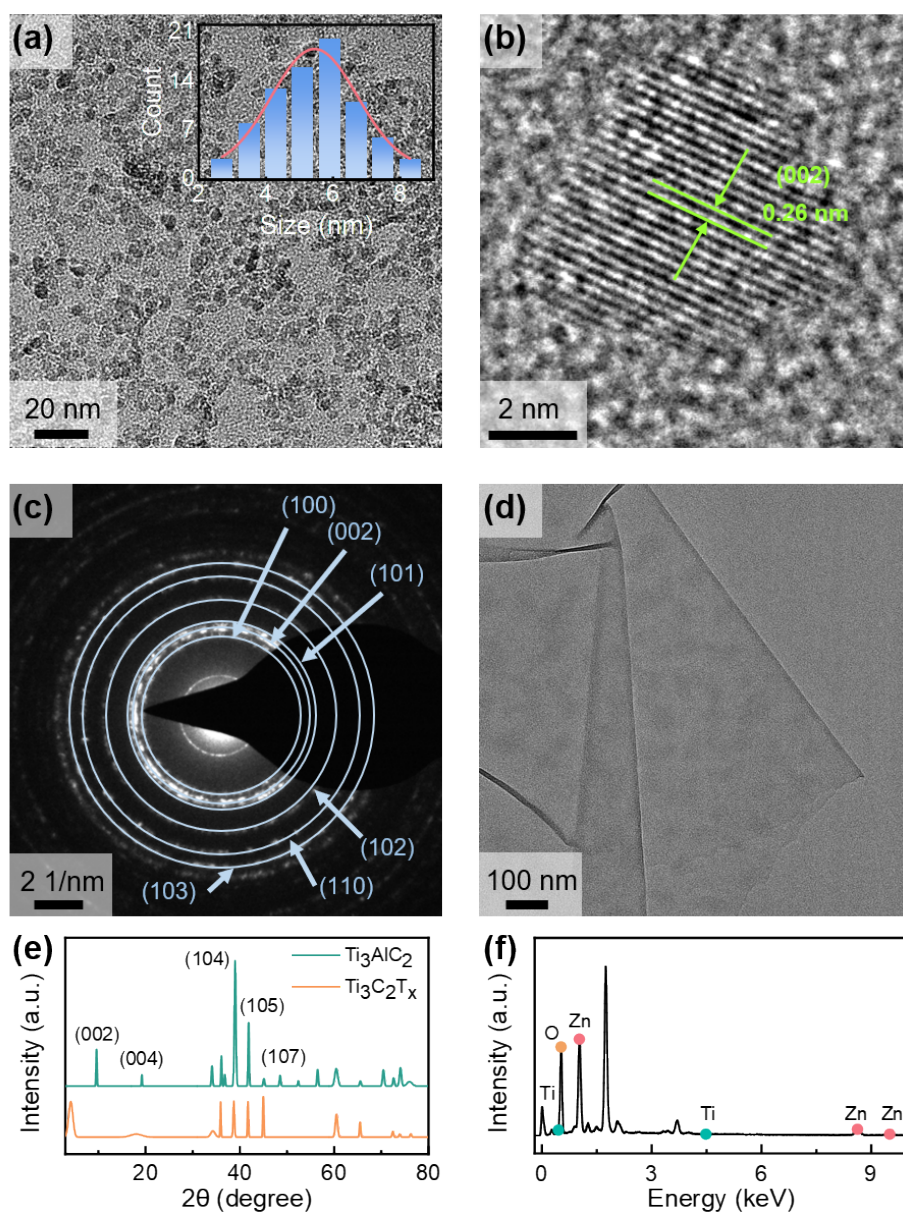


Fig. S1. (a) Transmission electron microscopy (TEM) image, (b) high-resolution transmission electron microscopy (HRTEM) image, and (c) selected area electron diffraction (SAED) patterns of ZnO quantum dots (QDs). (d) TEM image of MXene nanosheet. (e) X-ray diffraction (XRD) patterns of Ti_3AlC_2 MAX and $\text{Ti}_3\text{C}_2\text{T}_x$ MXene. (f) Elemental analysis of the 0D/2D composite thin film performed with energy-dispersive X-ray spectroscopy (EDS).

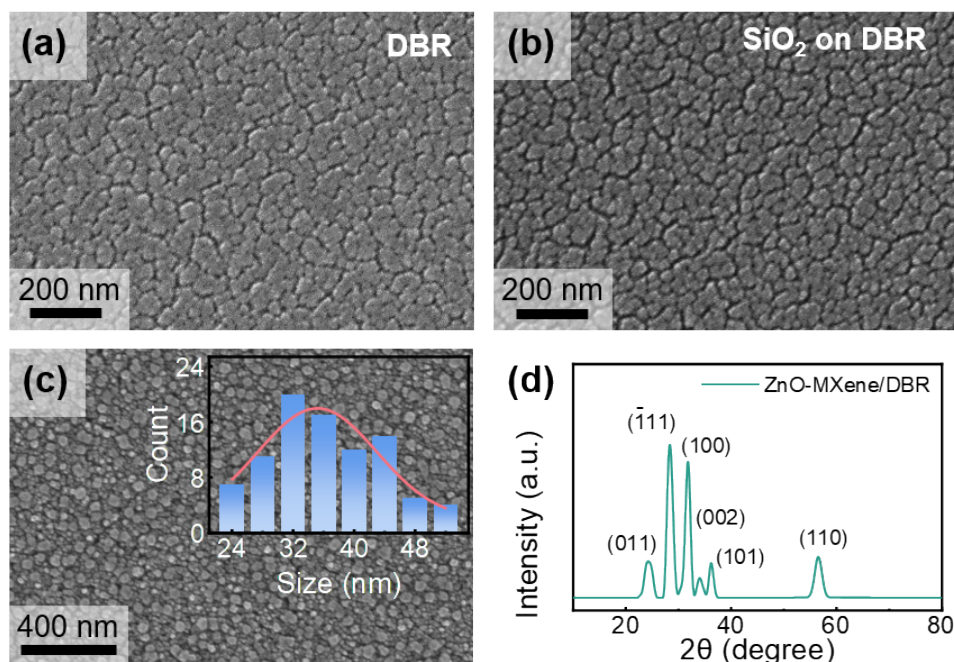


Fig. S2. Scanning electron microscopy (SEM) images of (a) DBR and (b) SiO₂ on DBR. (c) SEM image and (d) XRD patterns of the sample ZnO-MXene/DBR.

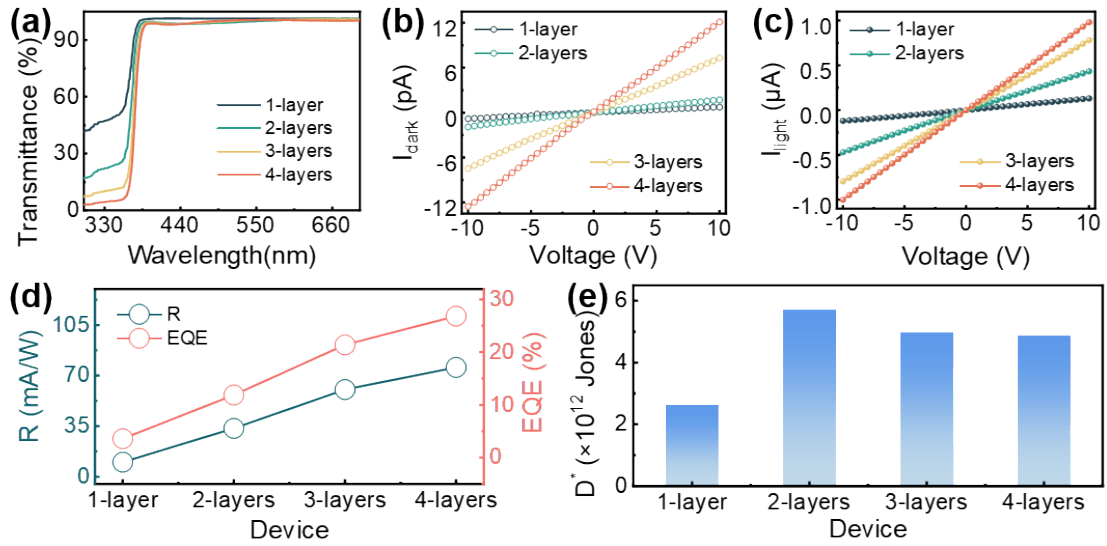


Fig. S3. (a) Transmittance spectra, (b) dark-current (I_{dark}), (c) photocurrent (I_{light}) of the devices with various layers of ZnO QDs. (d) Responsivity (R), external quantum efficiency (EQE), and **e** normalized detectivity (D^*) of the devices.

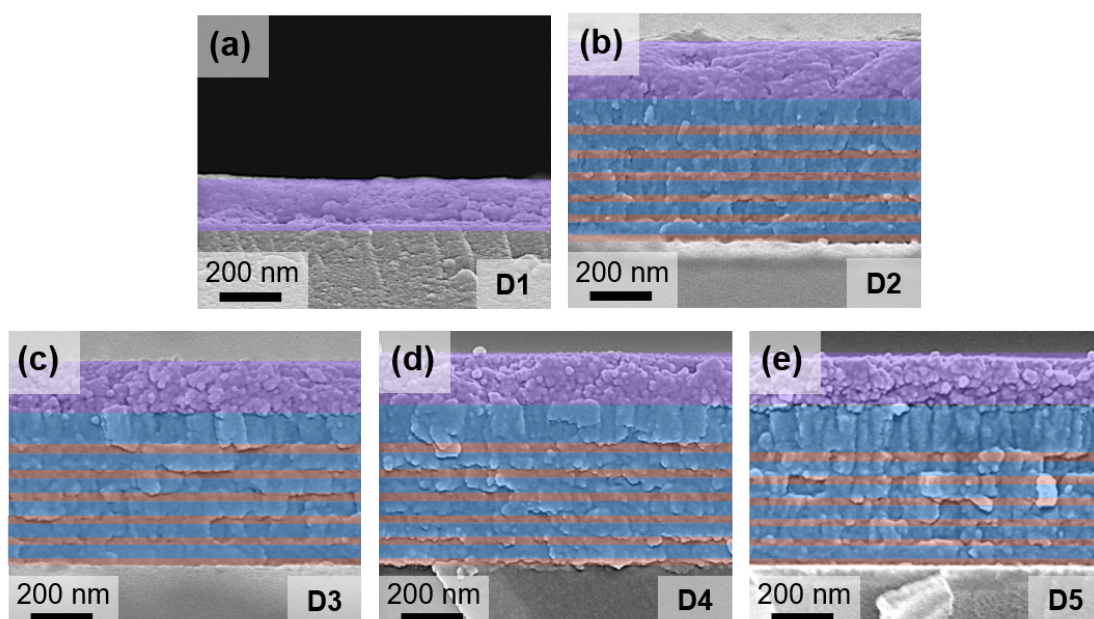


Fig. S4. Cross-sectional SEM images of the devices fabricated on (a) glass (D1) and on DBR with various thicknesses of SiO₂ isolating spacers: (b) 80 nm (D2), (c) 100 nm (D3), (d) 120 nm (D4), and (e) 140 nm (D5).

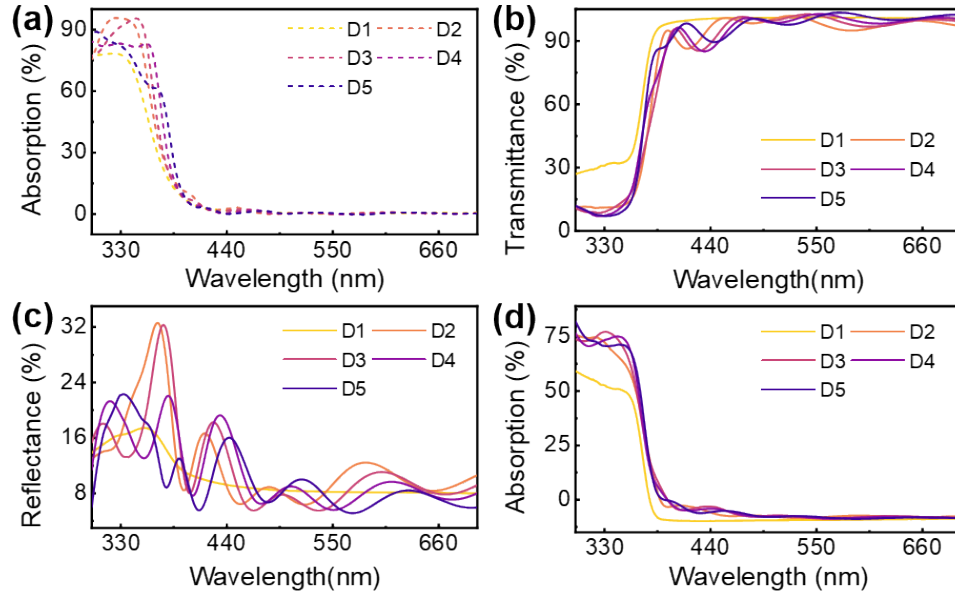


Fig. S5. (a) Simulated absorption spectra of the devices with various thicknesses of SiO₂ isolating spacers. (b) Transmittance, (c) reflectance, and (d) absorption spectra of the photodetectors.

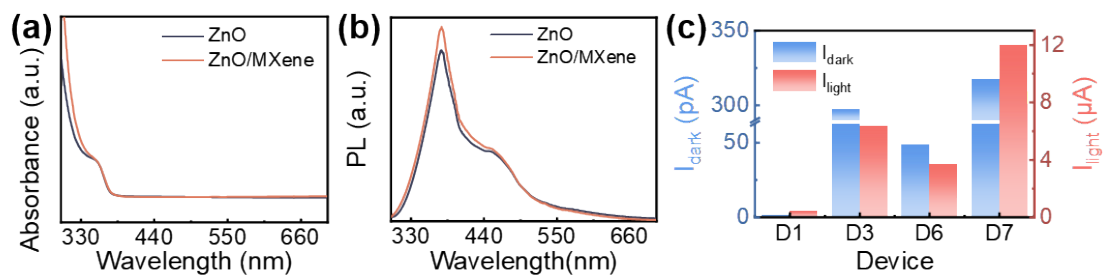


Fig. S6. (a) Absorbance and (b) photoluminescence (PL) spectra of ZnO QD and ZnO QD/MXene NS composite thin films. (c) I_{dark} and I_{light} of the devices at 10 V: ZnO/Glass (D1), ZnO/DBR (D3), ZnO-MXene/Glass (D6), and ZnO-MXene/DBR (D7).

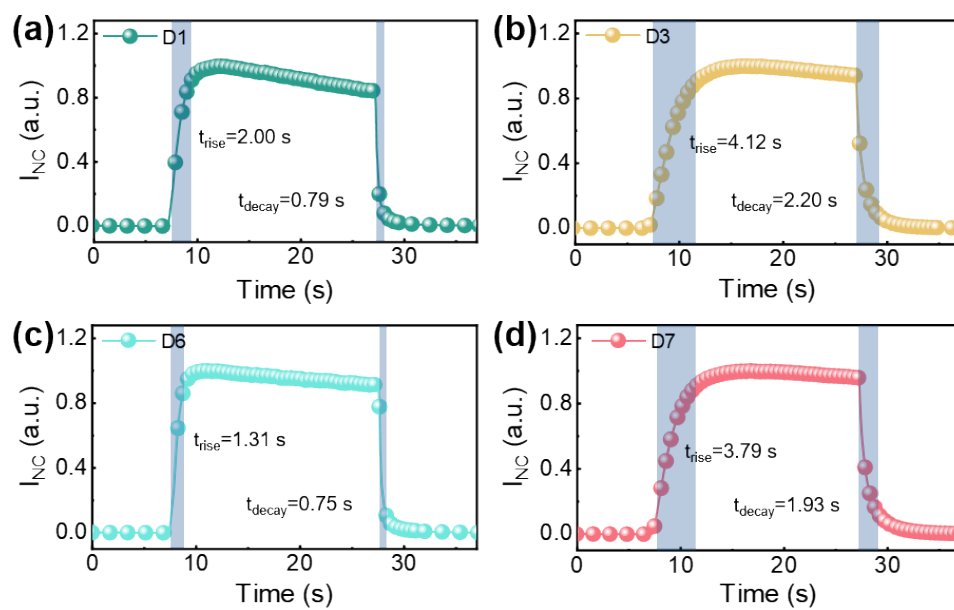


Fig. S7. Single period of the transient response of the photodetectors.

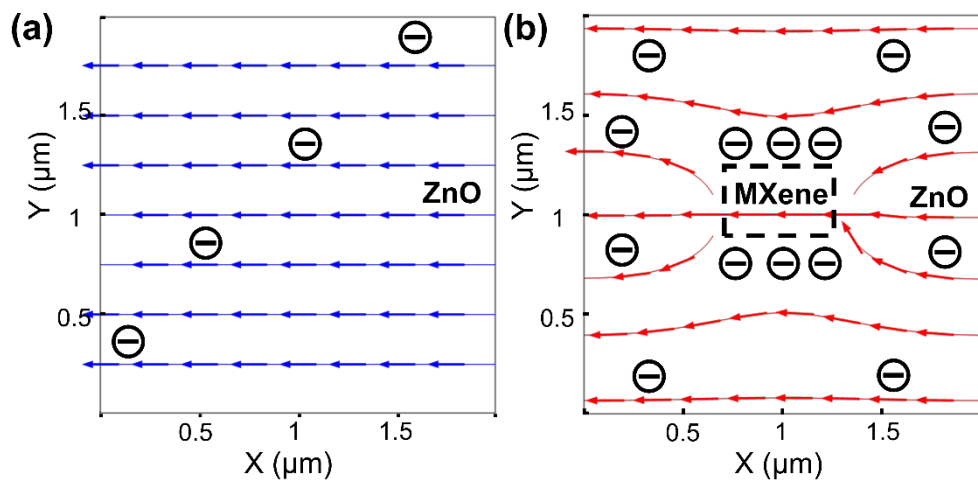


Fig. S8. Simulation of the current density distribution of (a) pristine ZnO and (b) ZnO QD/MXene NS nanocomposites.

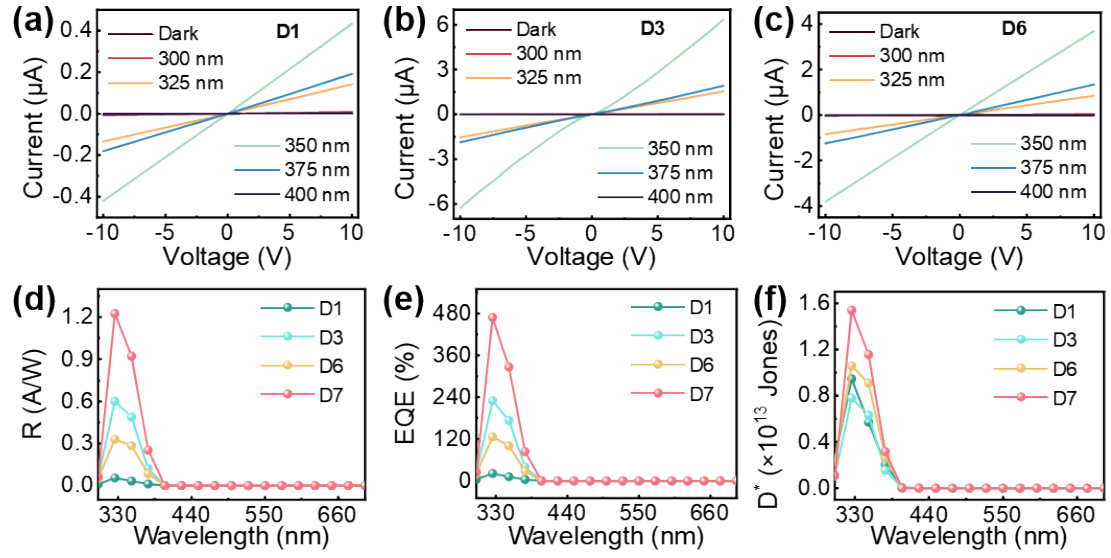


Fig. S9. (a) – (c) The I-V curves of the devices. The (d) R, (e) EQE, and (f) D^* of the photodetectors over a wavelength range between 300 and 700 nm.

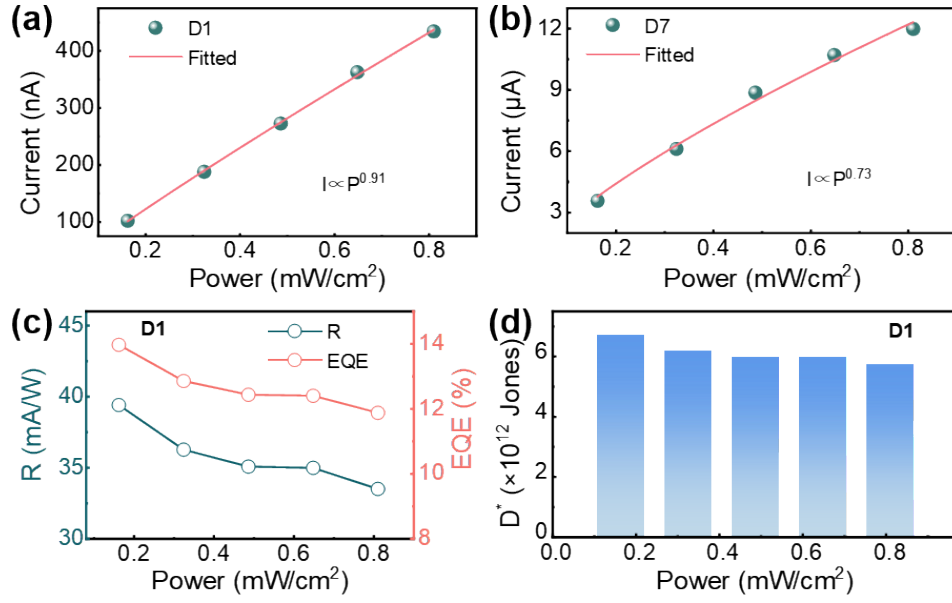


Fig. S10. Power law fitting curves of the device (a) D1 and (b) D7. The (c) R, EQE, and (d) D^* of the photodetector D1 with a variation of the light powers.

Table S1. Fitting coefficients and average lifetimes obtained from time-resolved photoluminescence (TRPL) spectra of the samples.

Sample	A_1	τ_1 (ns)	A_2	τ_2 (ns)	τ_{ave} (ns)
ZnO/Glass	0.40	0.42	0.61	0.99	0.87
ZnO-Mxene/Glass	0.83	0.34	0.17	1.78	1.09
ZnO/DBR	1.03	0.71	0.09	45.73	38.94

Table S2. R, EQE, and D* switching ratio (SR) of the devices with various layers of ZnO QDs.

Layers of ZnO	1-layer	2-layers	3-layers	4-layers
Transmittance at 350 nm	50.1%	24.3%	10.9%	4.7%
R	10.1	33.5	60.3	75.7
(mA W ⁻¹)				
EQE	3.6%	11.9%	21.4%	26.8%
D*	2.6	5.7	5.0	4.9
(×10 ¹² Jones)				
SR	1.8×10 ⁵	2.5×10 ⁵	1.1×10 ⁵	8.1×10 ⁴